

# Synthesis and Nicotinic Acetylcholine Receptor in Vitro and in Vivo Pharmacological Properties of 2'-Fluoro-3'-(substituted phenyl)deschloroepibatidine Analogues of 2'-Fluoro-3'-(4-nitrophenyl)deschloroepibatidine

Pauline Ondachi,<sup>†</sup> Ana Castro,<sup>‡</sup> Charles W. Luetje,<sup>‡</sup> M. Imad Damaj,<sup>§</sup> S. Wayne Mascarella,<sup>†</sup> Hernán A. Navarro,<sup>†</sup> and F. Ivy Carroll<sup>\*†</sup>

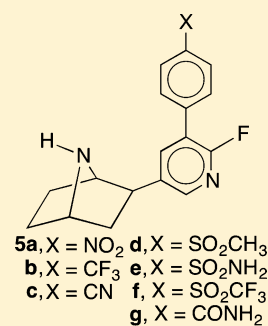
<sup>†</sup>Center for Organic and Medicinal Chemistry, Research Triangle Institute, P.O. Box 12194, Research Triangle Park, North Carolina 27709, United States

<sup>‡</sup>Department of Molecular and Cellular Pharmacology, Miller School of Medicine, University of Miami, Miami, Florida 33101, United States

<sup>§</sup>Department of Pharmacology and Toxicology, Virginia Commonwealth University Medical Campus, P.O. Box 980615, Richmond, Virginia 23298-0524, United States

**S** Supporting Information

**ABSTRACT:** Herein, we report the synthesis and nicotinic acetylcholine receptor (nAChR) in vitro and in vivo pharmacological properties of 2'-fluoro-3'-(substituted phenyl)deschloroepibatidines **5b–g**, analogues of 3'-(4-nitrophenyl) compound **5a**. All compounds had high affinity for  $\alpha 4\beta 2$ -nAChR and low affinity for  $\alpha 7$ -nAChR. Initial electrophysiological studies showed that all analogues were antagonists at  $\alpha 4\beta 2$ -,  $\alpha 3\beta 4$ -, and  $\alpha 7$ -nAChRs. The 4-carbamoylphenyl analogue **5g** was highly selective for  $\alpha 4\beta 2$ -nAChR over  $\alpha 3\beta 4$ - and  $\alpha 7$ -nAChRs. All the analogues were antagonists of nicotine-induced antinociception in the tail-flick test. Molecular modeling docking studies using the agonist-bound form of the X-ray crystal structure of the acetylcholine binding protein suggested several different binding modes for epibatidine, varenicline, and **5a–g**. In particular, a unique binding mode for **5g** was suggested by these docking simulations. The high binding affinity, in vitro efficacy, and selectivity of **5g** for  $\alpha 4\beta 2$ -nAChR combined with its nAChR functional antagonist properties suggest that **5g** will be a valuable pharmacological tool for studying the nAChR and may have potential as a pharmacotherapy for addiction and other central nervous system disorders.



Tobacco use is the leading preventable cause of disease, disability, and death in the United States. According to the Centers for Disease Control (CDC) 2011 Smoking & Tobacco Use Fact Sheet,<sup>1</sup> cigarette smoking results in more than 440 000 premature deaths in the United States each year—about 1 in every 5 deaths.

The continued use of tobacco products is believed to be due in large part to addiction to nicotine (1). It is well documented that nicotinic acetylcholine receptors (nAChRs) are the body's targets for nicotine actions. Considerable research suggests that  $\alpha 4\beta 2$ -nAChRs, the most abundant subtype in the brain, play a central role in nicotine addiction.<sup>2–4</sup> Human genetic association studies have also implicated  $\alpha 3$  (CHRNA3),  $\alpha 5$  (CHRNA5), and  $\beta 4$  (CHRNB4) nAChR subunits in nicotine-dependent subjects.<sup>5–7</sup> In addition, recent evidence from animal studies suggests that  $\alpha 3\beta 4$ -nAChRs may also contribute to nicotine's addictive properties<sup>2–4,8–10</sup> as well as reduction of ethanol consumption.<sup>11</sup> The association of nicotine with both  $\alpha 4\beta 2$ - and  $\alpha 3\beta 4$ -nAChRs in the addictive process makes these receptors attractive targets to combat nicotine addiction.

Even though nicotine dependence has a huge impact on global health, pharmacotherapies for treating tobacco use are limited.

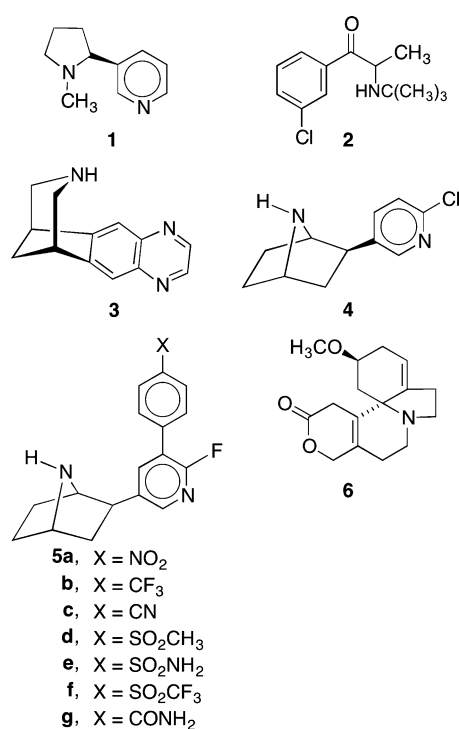
Food and Drug Administration (FDA)-approved therapies include nicotine-replacement therapies (NRTs), bupropion (2), and varenicline (3). Since only about one-fifth of smokers are able to maintain long-term (12 months) abstinence with any of the present pharmacotherapies,<sup>12,13</sup> new and improved drugs are needed.

During the past few years, we have conducted structure–activity relationship (SAR) studies using the potent nAChR agonist epibatidine (4) as a lead structure to identify agonist and antagonist pharmacophores for the nAChR.<sup>14–20</sup> In addition, we hoped that the studies would provide lead structures for the development of pharmacotherapies useful for treating smokers. In one of our studies we identified 2'-fluoro-3'-(4-nitrophenyl)-deschloroepibatidine (**5a**), also referred to as RTI-7527-102 and 4-nitro-PFEB, as a very high affinity nAChR ligand, which showed potent antagonism of nicotine-induced antinociception in the tail-flick and hot-plate tests.<sup>17</sup> In vitro testing of **5a** showed that it was a competitive antagonist of human  $\alpha 4\beta 2$ -nAChRs with a potency 17-fold higher than that of dihydro- $\beta$ -erythroidine (6) and lower potency at  $\alpha 3\beta 4$ - and  $\alpha 7$ -nAChRs.<sup>21</sup> In addition, the  $\alpha 4\beta 2$ -nAChR

Received: April 24, 2012

Published: June 28, 2012

antagonist **5a** attenuated the discriminative stimulus effects of nicotine, reduced nicotine's ability to facilitate intracranial self-stimulation (ICSS), blocked conditioned place preference (CPP) produced by nicotine, and dose-dependently blocked intravenous (iv) nicotine self-administration in rodents.<sup>22</sup> Thus, **5a** has both in vitro and in vivo properties thought to be favorable for a potential pharmacotherapy to treat smokers. Unfortunately, **5a** has a nitro-substituted phenyl group, a system that is associated with toxicity via partial reduction in vivo to the hydroxylamine, which can undergo metabolic activation to an electrophilic nitroso species. In this study we report the synthesis and nAChR in vitro and in vivo properties of **5b–g**, compounds which have the 4-nitro group in **5a** replaced by other strong electron-withdrawing groups. Computational chemistry studies were performed to compare the possible binding interactions of the 4-substituents of **5a–g** within a model of the nicotinic receptor.



## CHEMISTRY

**Synthesis of Compounds.** Scheme 1 outlines the synthesis used to prepare **5b–e**. Treatment of **7**<sup>17</sup> with di-*tert*-butyl

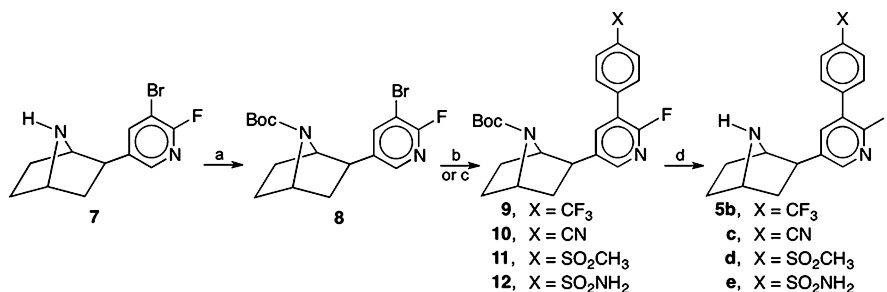
dicarbonate in methylene chloride containing triethylamine at room temperature overnight gives *tert*-butylcarbonyl-protected intermediate **8**. Suzuki cross-coupling of **8** with 4-(trifluoromethyl)phenylboronic acid, 4-(methylsulfonyl)phenylboronic acid, and 4-cyanophenylboronic acid in the presence of palladium diacetate, tris(*o*-tolyl)phosphine, and sodium carbonate in a dimethoxyethane–water mixture at 85 °C yielded **9**, **10**, and **11**. In the case of the synthesis of **12**, a Suzuki cross-coupling of **8** was conducted with the 4-boronobenzenesulfonamide through a microwave-assisted reaction in the presence of [1,1'-bis(diphenylphosphino)ferrocene]palladium(II) dichloride [PdCl<sub>2</sub>(dppf)] as a catalyst, potassium carbonate as a base, and 1,4-dioxane and water as solvents. The reaction was irradiated at 140 °C for 20 min to provide **12**. Treatment of **9–12** with trifluoroacetic acid in methylene chloride yielded **5b–e**. The synthesis of **5f** is given in Scheme 2. Suzuki–Miyaura borylation of **8** was performed through a microwave-assisted cross-coupling with bis(pinacolato)diboron in the presence of the weak base potassium acetate and PdCl<sub>2</sub>(dppf) as a catalyst, and the resulting material was irradiated at 140 °C for 15 min to furnish the boronic ester **13**. Suzuki cross-coupling of **13** with 4-bromophenyl trifluoromethyl sulfone (**15**) [prepared by the oxidation of commercially available 4-bromo[(trifluoromethyl)thio]benzene (**14**) with *m*-chloroperoxybenzoic acid (MCPBA)] afforded **16**, which on treatment with trifluoroacetic acid gave **5f**.

Compound **5g** was synthesized as shown in Scheme 3. Tetrakis(triphenylphosphine)palladium-catalyzed coupling of **7** with 4-carbamoylphenylboronic acid in dioxane–water containing potassium carbonate yielded **5g**. It should be noted that **5a–g** are all racemic analogues of epibatidine.

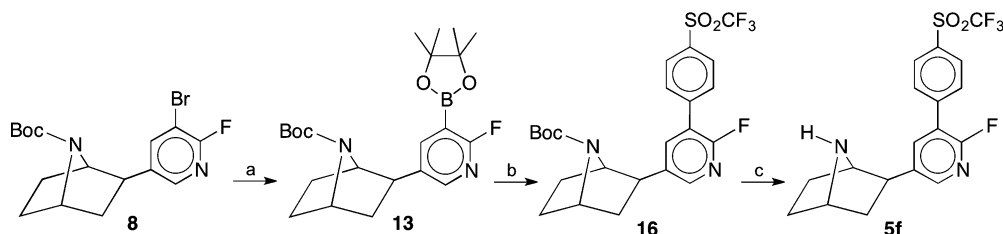
**Molecular Modeling.** To confirm that the nAChR could accommodate the structure and to explore the possible functional similarities to epibatidine of the proposed target compounds, each was examined in a series of ligand–receptor docking simulations. The model of the nAChR epibatidine binding pocket used in these calculations was based on the recently deposited X-ray crystallographic structure of a *Lymanaea stagnalis* acetylcholine binding protein (Ls-AChBP) chimera cocrystallized with epibatidine.<sup>23</sup> AChBP is considered a close structural analogue of nicotinic acetylcholine receptors, and this humanized Ls-AChCP chimera was selected as it was expected to have greater relevance to the mammalian receptor.

Docking calculations were performed using the Surflex-Dock module of the Tripos Sybyl molecular modeling program suite.<sup>24</sup> This system performs unbiased, conformationally independent docking of candidate ligands to proteins, which allows full flexibility of both the ligand and receptor side chains. An empirical scoring function (based on the Hammerhead docking system)

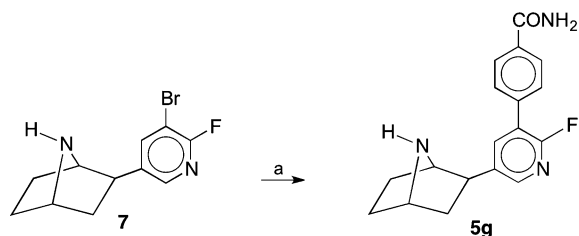
Scheme 1<sup>a</sup>



<sup>a</sup>Reagents and conditions: (a) (Boc)<sub>2</sub>O, Et<sub>3</sub>N, CH<sub>2</sub>Cl<sub>2</sub>, rt, overnight; (b) Pd(OAc)<sub>2</sub>, P(*o*-tolyl)<sub>3</sub>, Na<sub>2</sub>CO<sub>3</sub>, DME, H<sub>2</sub>O, 85 °C, XB(OH)<sub>2</sub> (X = CF<sub>3</sub>, CN, or SO<sub>2</sub>CH<sub>3</sub>); (c) PdCl<sub>2</sub>(dppf), K<sub>2</sub>CO<sub>3</sub>, 1,4-dioxane, H<sub>2</sub>O, microwave, 140 °C, 20 min; (d) CF<sub>3</sub>CO<sub>2</sub>H, CH<sub>2</sub>Cl<sub>2</sub>.

Scheme 2<sup>a</sup>

<sup>a</sup>Reagents and conditions: (a) bis(pinacolato)diboron, KOAc, PdCl<sub>2</sub>(dppf), 1,4-dioxane, microwave, 140 °C, 20 min; (b) Pd(PPh<sub>3</sub>)<sub>4</sub>, K<sub>2</sub>CO<sub>3</sub>, DME–EtOH–H<sub>2</sub>O, microwave, 140 °C, 20 min, 4-BrC<sub>6</sub>H<sub>4</sub>SO<sub>2</sub>CF<sub>3</sub> (15) (prepared by oxidation of 4-BrC<sub>6</sub>H<sub>4</sub>SCF<sub>3</sub> (14) with MCPBA); (c) CF<sub>3</sub>CO<sub>2</sub>H, CH<sub>2</sub>Cl<sub>2</sub>.

Scheme 3<sup>a</sup>

<sup>a</sup>Reagents and conditions: (a) Pd(PPh<sub>3</sub>)<sub>4</sub>, K<sub>2</sub>CO<sub>3</sub>, 1,4-dioxane, H<sub>2</sub>O, reflux, 24 h with 4-carbamoylphenylboronic acid.

is used to select likely binding modes and conformations. The scoring function includes steric, polar, entropic, and solvation terms to estimate the binding affinity of each docked ligand.

## RESULTS

**Biological.** The nAChR binding affinities and the functional nicotinic pharmacological properties of 2'-fluoro-3'-(substituted phenyl)deschloroepibatidine analogues **5a–g** were determined. The  $K_i$  values for the inhibition of [<sup>3</sup>H]epibatidine and [<sup>125</sup>I]iodoMLA binding at the  $\alpha 4\beta 2^*$ - and  $\alpha 7$ -nAChRs, respectively, for **5b–g** along with reference compounds nat-epibatidine (**4**) and varenicline (**3**) and the lead compound **5a** are listed in Table 1. The reference standards nat-epibatidine and varenicline and lead compound **5a** have  $K_i$  values of 0.026, 0.12, and 0.009 nM for the  $\alpha 4\beta 2^*$ -nAChR, respectively. Similar to **5a**, **5b–g** with  $K_i$  values ranging from 0.03 to 0.94 nM had high affinity for  $\alpha 4\beta 2^*$ -nAChR. The 4-[(trifluoromethyl)sulfonyl]phenyl analogue **5f** with a  $K_i$  of 0.03 nM had the highest affinity. Similar to lead compound **5a**, **5b–g** had weak affinity for the  $\alpha 7$ -nAChR ( $K_i > 2 \mu\text{M}$ ). In a preliminary study using inhibition of [<sup>3</sup>H]epibatidine and stably transfected nAChR cell lines, Huang et al.<sup>25</sup> reported that **5c** had  $\alpha 4\beta 2$ -nAChR selectivity relative to five other  $\alpha\beta$ -nAChRs.

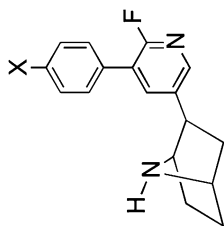
The nAChR subtype selectivity of **5b–g**, as well as nat-epibatidine, varenicline, and lead compound **5a**, was assessed in an initial electrophysiological assay using  $\alpha 4\beta 2$ -,  $\alpha 3\beta 4$ -, and  $\alpha 7$ -nAChRs expressed in *Xenopus* oocytes (Table 1). The current response to a high concentration (100  $\mu\text{M}$ ) of each compound was compared to the maximum response that can be achieved with acetylcholine. Compounds **5a–f** lacked agonist activity at  $\alpha 4\beta 2$  in this initial screen, while **5g** had a low level of agonist activity at this subtype. Compounds **5b** and **5d,e** lacked agonist activity at  $\alpha 3\beta 4$ , while **5a**, **5c**, **5f**, and **5g** had a low level of agonist activity at this subtype. At  $\alpha 7$ -nAChRs, **5a–f** displayed low levels of agonist activity, while **5g** showed a moderate level

of agonist activity (17  $\pm$  4% of the maximal ACh response). As an initial screen of antagonist properties, we measured the current response to an EC<sub>50</sub> concentration of acetylcholine in the presence of a 100  $\mu\text{M}$  concentration of each compound and compared this to a preceding current response to acetylcholine alone. Compounds **5a–g** were found to be antagonists at the  $\alpha 4\beta 2$ -,  $\alpha 3\beta 4$ -, and  $\alpha 7$ -nAChR subtypes. The results from this initial screen suggested that this compound series manifested a variety of desirable functional selectivities:  $\alpha 4\beta 2$ - and  $\alpha 3\beta 4$ -nAChRs over  $\alpha 7$ -nAChR and  $\alpha 4\beta 2$ -nAChR over  $\alpha 3\beta 4$ - and  $\alpha 7$ -nAChRs. We examined the subtype selectivity of antagonist activity for some of these compounds (**5a–d** and **5g**) in more detail by generating concentration–inhibition curves (Table 2). Compound **5b** showed no selectivity among  $\alpha 4\beta 2$ -,  $\alpha 3\beta 4$ -, and  $\alpha 7$ -nAChRs. Compounds **5a** and **5d** showed a moderate selectivity for  $\alpha 4\beta 2$ -nAChR over  $\alpha 3\beta 4$ -nAChR (2.5-fold and 4-fold, respectively) and a greater selectivity for  $\alpha 4\beta 2$ -nAChR over  $\alpha 7$ -nAChR (10-fold in each case). Compound **5c** showed similar antagonist potency at  $\alpha 4\beta 2$  and  $\alpha 3\beta 4$  and was less potent at  $\alpha 7$  (9-fold and 14-fold, respectively). Compound **5g** was highly selective for  $\alpha 4\beta 2$ - over  $\alpha 3\beta 4$ -nAChRs and  $\alpha 7$ -nAChR (23-fold in each case).

Similar to varenicline, the lead compound **5a** had no functional activity in the mouse tail-flick and hot-plate tests but had agonistic effects with ED<sub>50</sub> values of 0.21 and 0.22 mg/kg in the hypothermia and spontaneous activity assays compared to 2.8 and 2.1 mg/kg in these two tests for varenicline. None of the analogues **5b–g** had activity in the tail-flick and hot-plate tests. Analogues **5b**, **5c**, **5d**, and **5e** also had no activity in the hypothermia and spontaneous activity tests. Analogue **5f** was only active in the spontaneous activity test. Similar to **5a** and varenicline, **5g** was only active in the hypothermia and spontaneous activity tests. The discrepancy between the high binding affinity of **5a–g** for  $\alpha 4\beta 2^*$ -nAChRs and their absence of agonistic effects in the pain tests suggests that these compounds might act as functional nAChR antagonists in the two pain tests. Indeed, all the compounds were antagonists of nicotine-induced antinociception in the tail-flick test, with AD<sub>50</sub> values ranging from 0.9  $\mu\text{g}/\text{kg}$  for **5e** to 38  $\mu\text{g}/\text{kg}$  for **5b**. Compounds **5b**, **5d**, and **5e** were also antagonists in the hot-plate test. Compound **5e** with AD<sub>50</sub> values of 0.9 in the tail-flick test was more potent than **5a** in this assay. Overall, these acute mouse results suggest that **5b**, **5c**, **5d**, and **5e** are nAChR antagonists and **5a**, **5g**, and **5f** are weak partial agonists.

**Molecular Modeling.** The results of these docking studies for **5a–g** (Corey–Pauling–Koltun (CPK) atom-type coloring scheme) and varenicline (“Var”) compared to the observed binding mode of epibatidine (“Epi”) are shown in Figure 1. The “total” docking scores (an estimated  $-\log(K_d)$ ), as calculated

**Table 1.** Comparison of Epibatidine and Varenicline Radioligand Binding, Antinociception, and in Vitro Functional Data to Those of 2'-Fluoro-3'-(substituted phenyl)deschloroepibatidine Analogues



compd <sup>a</sup>	X	$\alpha_7$ [ <sup>125</sup> I] iodoMLA $K_i$ (nM) (Hill slope)	$\alpha_7$ [ <sup>3</sup> H] epibatidine $K_i$ (nM) (Hill slope)	ED <sub>50</sub> tail flick (mg/kg)	ED <sub>50</sub> hot plate (mg/kg)	ED <sub>50</sub> hypothermia (mg/kg)	ED <sub>50</sub> spontaneous activity (mg/kg)	AD <sub>50</sub> ( $\mu$ g/kg)			agonist activity (% max ACh Ach response remaining at 100 $\mu$ M compd)			antagonist activity (% EC <sub>50</sub> Ach response remaining at 100 $\mu$ M compd)			
								tail flick	hot plate	tail flick	$\alpha 4/\beta 2$	$\alpha 3/\beta 4$	$\alpha 7$	$\alpha 4/\beta 2$	$\alpha 3/\beta 4$	$\alpha 7$	
nat-epibatidine			0.026 $\pm$ 0.002	0.006 (0.001–0.01)	0.004 (0.001–0.008)	0.004 (0.002–0.008)	0.001 (0.0005–0.005)	131 $\pm$ 13	97 $\pm$ 4	150 $\pm$ 8	nd	nd	nd	nd	nd	nd	
varenicline								470									
<b>5a</b>	NO <sub>2</sub>	32.5 $\pm$ 1.3	>2000	11% at 10	10% at 10	2.8	2.1	0.2	13 $\pm$ 0.4	66 $\pm$ 4	74 $\pm$ 5	38 $\pm$ 2	nd	nd	nd	nd	
				5% at 10	10% at 10	0.21 (0.4–1.9)	0.22 (0.04–1.2)	3 (0.8–45)	0	4 $\pm$ 1	6 $\pm$ 1	6 $\pm$ 1	9 $\pm$ 2	55 $\pm$ 6			
<b>5b</b>	CF <sub>3</sub>	>2000	>2000	4% at 10	6% at 10	0% at 10	5% at 10	38 (2–50)	6000 (4100–8800)	0	4 $\pm$ 1	8 $\pm$ 2	4 $\pm$ 1	3 $\pm$ 1			
<b>5c</b>	CN	>2000	>2000	4% at 10	18% at 10	0% at 10	0% at 10	6 (3–100)	24% at 10000	0	6 $\pm$ 1	8 $\pm$ 2	17 $\pm$ 2	49 $\pm$ 5			
<b>5d</b>	CH <sub>3</sub> SO <sub>2</sub>	>2000	>2000	6% at 10	1% at 10	1% at 10	12% at 10	18 (2–160)	2600 (1100–5800)	0	3 $\pm$ 1	10 $\pm$ 3	25 $\pm$ 5	33 $\pm$ 2			
<b>5e</b>	H <sub>3</sub> NSO <sub>2</sub>	>2000	>2000	4% at 10	19% at 10	0% at 10	5% at 10	0.9 (0.4–1.8)	1000 (100–1800)	0	1.8 $\pm$ 0.5	4 $\pm$ 1	5 $\pm$ 2	18 $\pm$ 2			
<b>5f</b>	CF <sub>3</sub> SO <sub>2</sub>	>2000	>2000	3% at 10	15% at 10	0% at 10	4.2 (1–16)	1600 (1500–1800)	50% at 10000	0	1.9 $\pm$ 0.6	1.8 $\pm$ 0.4	7 $\pm$ 2	15 $\pm$ 5	42 $\pm$ 5		
<b>5g</b>	CONH <sub>2</sub>	1870 $\pm$ 298	16% at 10	60% at 10	4.2 (1.5–11.6)	3.5 (1–11.3)	9 (3–31)	1% at 2000	3.5 $\pm$ 1.1	8 $\pm$ 1	17 $\pm$ 4	6 $\pm$ 1	36 $\pm$ 4	54 $\pm$ 5			

<sup>a</sup>All compounds were tested as their (±)-isomers. <sup>b</sup>The  $K_i$  for (±)-[<sup>3</sup>H]epibatidine is 0.02 nM.

**Table 2. Comparison of Antagonist Potency ( $IC_{50}$  Values) for Several 2'-Fluoro-3'-(substituted phenyl)deschloroepibatidine Analogues**

compd	antagonist activity $IC_{50}$ ( $\mu M$ )		
	$\alpha 4\beta 2$	$\alpha 3\beta 4$	$\alpha 7$
varenicline	$0.20 \pm 0.03^a$		
5a	$3.2 \pm 0.2$	$7.9 \pm 0.5$	$32 \pm 12$
5b	$6.0 \pm 0.4$	$5.0 \pm 0.3$	$4.0 \pm 0.8$
5c	$11 \pm 1$	$7 \pm 7$	$98 \pm 13$
5d	$2.8 \pm 0.4$	$11 \pm 2$	$19 \pm 7$
5g	$1.5 \pm 0.1$	$35 \pm 7$	$35 \pm 12$

<sup>a</sup>Data were taken from ref 29.

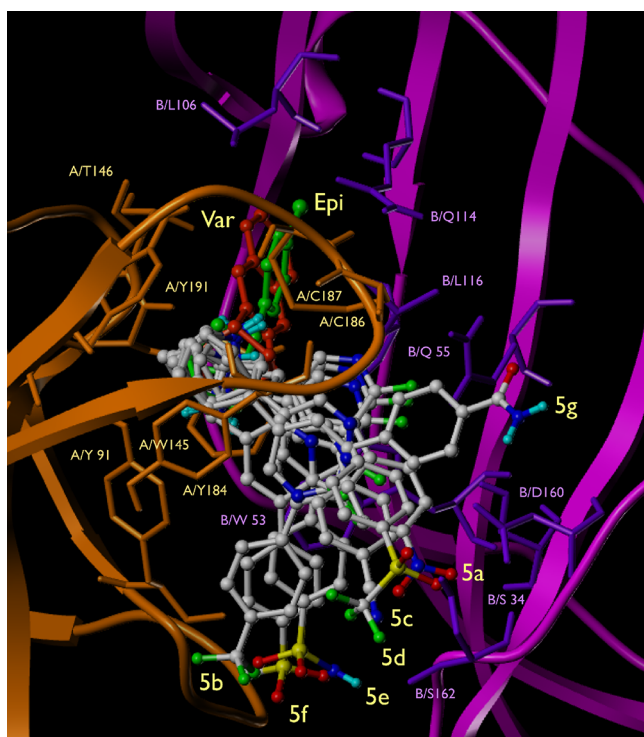


**Figure 1.** Overlay of the calculated docking geometries of 5a–g and varenicline overlaid with the observed X-ray crystallographic structure of epibatidine cocrystallized with an  $\alpha 7$ -AChBP chimera (PDB 3SQ6). The “A” subunit of the receptor (the C-loop region) is colored orange and the “B” subunit purple. Epibatidine is colored green and varenicline red, and the 5a–g epibatidine analogues are rendered with CPK atom-type colors.

with the Tripos CScore module, were used to select the optimal binding geometries. The CScore total docking scores for this series were (5a) 7.55, (5b) 7.53, (5c) 6.74, (5d) 7.36, (5e) 9.02, (5f) 7.46, and (5g) 9.40. All of the observed and predicted binding geometries share a common feature: the cationic azabicyclic ring of each ligand is centered in the electron-rich pocket formed by a cluster of five aromatic residues (A/TYR91, A/TRP145, A/TYR184, A/TYR191, B/TRP53). (This binding pocket is also bordered by the hydrophobic A/CYS186, A/CYS187, and B/LEU116 residues.) In addition, a hydrogen bond interaction within the aromatic pocket between the ligand and either A/TRP145 (backbone carbonyl) or the adjacent A/TYR91 (side chain hydroxyl) is observed or predicted for all ligands (the observed structure of the epibatidine–receptor complex and the computationally docked varenicline binding

geometry exhibit both). By pivoting around these common anchoring interactions, four distinct binding modes are exhibited (by epibatidine) or predicted (for 5a–g and varenicline). In binding mode 1, the smaller ligands, epibatidine and varenicline, associate with a relatively small pocket formed by B/LEU116, B/GLN114, B/LEU106, and A/TRP146 (Figure 2A). Compounds 5a–g are too large to fit into this pocket and thus are predicted to interact with the receptor differently compared with the parent compound epibatidine or varenicline. In binding mode 2 (Figure 2B), compounds 5a, 5c, and 5d associate with the aforementioned aromatic pocket and, in addition, the ligand polar substituents interact with a relatively polar receptor pocket bordered by B/SER162, B/GLY163, B/ASP160, and B/SER34. In the case of 5a, additional hydrogen bond interactions with B/GLY163 and B/GLN55 are suggested by the docking simulation. A hydrogen bond interaction between the ligand pyridinyl nitrogen and B/GLN55 is also predicted for compound 5c. Compounds 5b, 5e, and 5f are predicted to have a slightly different binding mode (Figure 2C) where the para substituent is situated in the large cavity between the base of the C-loop and B/SER162. In this set of three epibatidine analogues, additional hydrogen bonds are predicted involving B/GLY163 (5e and 5f) and A/TRP45, B/SER162, B/GLY163, and B/GLN55 (5f). A unique, fourth binding mode is predicted for compound 5g (Figure 2D). The docking simulation for this compound predicts that the 4-acetamido substituent will be situated in a polar pocket bordered by B/SER32, B/ASP160, and B/GLN55 where it forms a salt bridge with B/ASP160. This interaction, unique to 5g, accounts for the very favorable predicted  $pK_d$  of 9.40, the highest for the series.

## DISCUSSION

In previous studies we showed that the addition of a 3'-substituent to epibatidine, 2'-fluoroepibatidine, or deschloroepibatidine provided analogues with different degrees of nAChR functional agonist and antagonist properties.<sup>14–17,19,26</sup> All 2'-fluoro-3'-(substituted phenyl)deschloroepibatidine analogues possessed high affinity for  $\alpha 4\beta 2^*$ -nAChRs. Compound 5a, with a  $K_i = 0.009$  nM compared to a  $K_i = 0.026$  nM for natepibatidine, had the highest affinity.<sup>17</sup> Thus, a bulky substituted phenyl group at the 3'-position does not interfere with receptor recognition for the  $\alpha 4\beta 2^*$ -nAChRs. All analogues were potent antagonists. Thus, a 2'-fluoro group on the pyridine ring combined with bulky 3'-substituents interferes with receptor activation. Several 2'-fluoro-3'-(substituted phenyl)-deschloroepibatidine analogues were evaluated for  $\alpha 4\beta 2$  potency and selectivity in cloned nAChRs.<sup>21</sup> The 3'-(4-nitrophenyl) analogue 5a was a more potent and selective competitive antagonist for the  $\alpha 4\beta 2$ -nAChR than dihydro- $\beta$ -erythroidine (6, DH $\beta$ E). Compound 5a was also evaluated in several animal models related to nicotine reward and reinforcement: drug discrimination (DD), intracranial self-stimulation (ICSS), conditioned place preference (CPP), and limited access to nicotine iv self-administration (SA).<sup>22</sup> All of these behavioral effects of nicotine are largely mediated by neuronal  $\alpha 4\beta 2^*$ -nAChRs. The antagonist 5a attenuated the DD effect of nicotine but alone failed to produce nicotine-like DD effects, reduced nicotine's ability to facilitate ICSS while producing no effects on ICSS alone, and blocked CPP produced by nicotine but alone failed to produce a CPP and dose-dependently blocked SA.<sup>22</sup> Results from these studies showed that 5a has the nAChR in vitro and in vivo

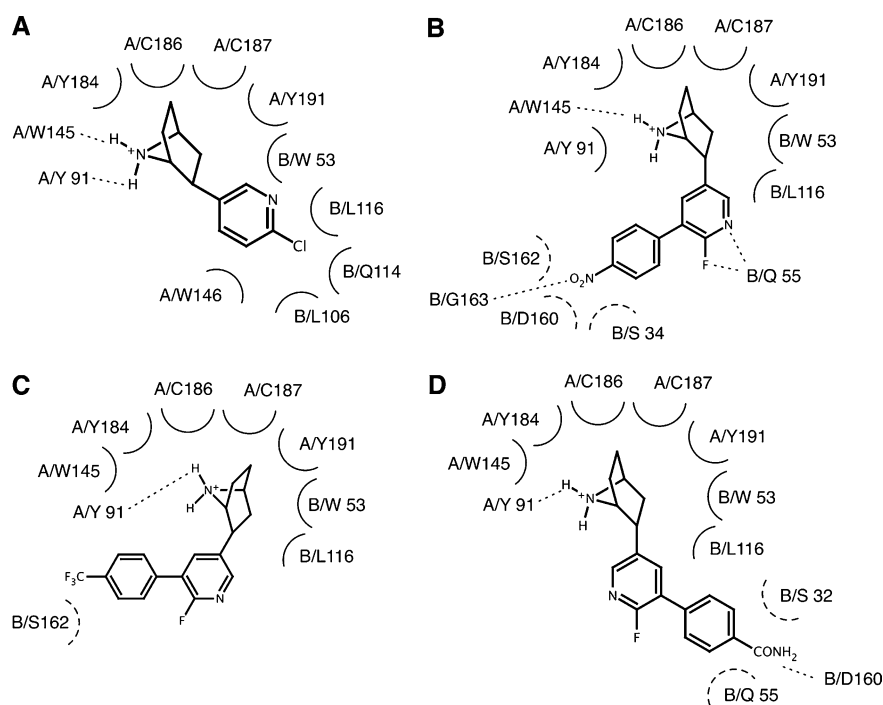


**Figure 2.** Diagrams of the salient ligand–receptor close contacts (5 Å cutoff) for epibatidine (observed) and **5a–g** and varenicline (calculated): (A) binding mode 1 (epibatidine and varenicline); (B) binding mode 2 (analogues **5a**, **5c**, and **5d**); (C) binding mode 3 (analogues **5b**, **5e**, and **5f**); (D) binding mode 4 (analogue **5g**).

pharmacological properties for a potential clinical candidate to treat nicotine dependence. Since **5a** has an aromatic nitro substituent that could be partially reduced to a hydroxylamine group *in vivo* which could undergo metabolite activation to an electrophilic nitroso species, resulting in toxic effects, its potential for drug development could be questioned. In this study we designed, synthesized, and evaluated the **5a** analogues **5b–g** for their *in vitro* and *in vivo* nAChR properties. Similar to lead structure **5a**, each compound has a strong electron-withdrawing 4-substituent on the 3'-aryl group. Table 3 lists the  $\sigma$  constants for **5a–g**.<sup>27</sup>

**Table 3. Comparison of Representative  $\sigma$  Constants Derived from Different Systems<sup>a</sup>**

substituent	$\sigma_m$	$\sigma_p$	$\sigma_p^0$	$\sigma_p^+$	$\sigma_p^-$	R	F
NO <sub>2</sub>	0.71	0.78	0.82	0.79	1.27	0.13	0.65
SO <sub>2</sub> NH <sub>2</sub>	0.53	0.60			0.94	0.11	0.49
CF <sub>3</sub>	0.43	0.54	0.54	0.61	0.65	0.16	0.38
SO <sub>2</sub> CF <sub>3</sub>	0.86	0.96	0.93		1.63	0.22	0.74
CN	0.56	0.66	0.68	0.66	1.00	0.15	0.51
CONH <sub>2</sub>	0.28	0.36			0.61	0.10	0.26
SO <sub>2</sub> CH <sub>3</sub>	0.60	0.72	0.75		1.13	0.19	0.53

<sup>a</sup>Data were taken from ref 27.

We evaluated the potency and selectivity of **5a–g** *in vitro* using three cloned nAChR subtypes ( $\alpha 4\beta 2$ ,  $\alpha 3\beta 4$ , and  $\alpha 7$ ) expressed in *Xenopus* oocytes and assayed using electrophysiology. While we found lead structure **5a** to be selective for  $\alpha 4\beta 2$  over  $\alpha 3\beta 4$ , the difference in potency (2.5-fold) was much less than previously reported.<sup>21</sup> In our electrophysiology assay in the current study, we used rat nAChR subunits to generate the nAChRs. In the previous study, human  $\alpha 4\beta 2$  was compared to rat  $\alpha 3\beta 4$ .<sup>21</sup> Thus, the difference in selectivity may be attributable to a difference between rat and human  $\alpha 4\beta 2$ .

Such pharmacological differences have been previously reported for rat and human  $\alpha 7$ .<sup>28</sup> Concentration–inhibition analysis showed **5b** to be nonselective for the nAChR subtypes tested. Compound **5d** was modestly selective for  $\alpha 4\beta 2$  over  $\alpha 3\beta 4$  and  $\alpha 7$ , while **5c** was moderately selective for  $\alpha 4\beta 2$  and  $\alpha 3\beta 4$  over  $\alpha 7$ . Interestingly, the greatest subtype selectivity was generated by placing a carbamoyl moiety at the 4-position (**5g**). Compound **5g** displayed 23-fold selectivity for  $\alpha 4\beta 2$  over  $\alpha 3\beta 4$  and  $\alpha 7$ . Molecular modeling docking studies of **5g** to the antagonist form of the AChBP suggests a binding mode that could account for the  $\alpha 4\beta 2$ -nAChR selectivity of **5g**.

While the functional selectivity of compound **5g** for  $\alpha 4\beta 2$  over  $\alpha 7$  is exciting, the degree of selectivity (23-fold) observed in the electrophysiological assay is much less than what we observed in the radioligand binding assays (>15000-fold). Similarly, while compounds **5a–d** showed a selectivity of 3–4 orders of magnitude for  $\alpha 4\beta 2$  over  $\alpha 7$  in radioligand binding assays, these compounds displayed only moderate selectivity (6–10-fold for **5a**, **5c**, and **5d**) or no selectivity (**5b**) in the electrophysiology assay. These findings are reminiscent of what was observed when comparing results for varenicline in radioligand binding and electrophysiological assays.<sup>29,30</sup> The reason for this difference is equilibrium binding assays and electrophysiological assays measure the properties of different receptor states. Unfortunately, the large differences in affinity observed in equilibrium binding assays are generally not observed in functional assays, and the rank order of affinities does not necessarily correlate with the rank orders of functional potency.<sup>31,32</sup>

In summary, several 2'-fluoro-3'-(substituted phenyl)-deschloroepibatidine analogues were developed which had high binding affinity for the  $\alpha 4\beta 2$ -nAChR. The high binding affinity and *in vitro* efficacy selectivity of the 3'-(4-carbamoylphenyl) analogue **5g** combined with its ability to antagonize nicotine-induced antinociception in the tail-flick test

suggest that this compound will be a valuable pharmacological tool for studying the nAChR and may have potential as a pharmacotherapy for addiction and other central nervous system (CNS) disorders. In addition, having these various compounds with a variety of selectivity profiles toward both  $\alpha 4\beta 2$ - and  $\alpha 3\beta 4$ -nAChR subtypes relative to the  $\alpha 7$ -nAChR provides the opportunity for manipulating these important pharmacological and therapeutic targets and allows for the evaluation of dual-acting nicotinic antagonists.

## EXPERIMENTAL SECTION

Melting points were determined on a Mel-temp (Laboratory Devices, Inc.) capillary tube apparatus. Nuclear magnetic resonance ( $^1\text{H}$  and  $^{13}\text{C}$  NMR) spectra were recorded at 300 MHz (Bruker Avance 300). Chemical shift data for the proton resonances are reported in parts per million ( $\delta$ ) relative to tetramethylsilane ( $\delta$  0.0) as an internal standard. Thin-layer chromatography was carried out on Whatman silica gel 60 plates. Visualization was accomplished under UV or in an iodine chamber. Microanalysis was carried out by Atlantic Microlab, Inc. The purity of the compounds (>95%) was established by elemental analysis. Flash chromatography was carried out using a CombiFlash Rf Teledyne Isco instrument and columns, silica gel 60 (230–400 mesh), and various solvent mixtures. Microwave reactions were carried out using a CEM Discover microwave reactor.

[ $^3\text{H}$ ]Epibatidine was purchased from Perkin-Elmer Inc. (Boston, MA). [ $^{125}\text{I}$ ]Iodo-MLA was synthesized as previously reported.<sup>33</sup>

**General Procedure for the Synthesis of Compounds 5b and 5c Hydrochlorides.** The respective Boc-protected compound (9 or 10) (0.7 mmol) was dissolved in anhydrous  $\text{CH}_2\text{Cl}_2$  (3 mL) and cooled in an ice–water bath. TFA (3 mL) was added over a 30 min period and the mixture stirred at rt for 1 h. The mixture was poured into a cold solution of  $\text{NH}_4\text{OH}$  in water (1:1) and was extracted with  $\text{CH}_2\text{Cl}_2$ . The organic phase was washed with brine, dried ( $\text{Na}_2\text{SO}_4$ ), and evaporated to dryness. The resulting residue was subjected to flash chromatography on a silica gel column using  $\text{CH}_2\text{Cl}_2$ –MeOH as the eluent to provide the respective amine (5b or 5c). Subsequently, the free base was dissolved in MeOH (5 mL) at room temperature, HCl (1 M in ether) added with a syringe pump over 50 min at room temperature, the mixture stirred for 30 min, and the solvent removed. The resulting residue was recrystallized from MeOH–ether to provide the hydrochloride salt.

**2'-Fluoro-3'-[4-(trifluoromethyl)phenyl]deschloroepibatidine (5b) Hydrochloride.** Data for 5b:  $^1\text{H}$  NMR ( $\text{CDCl}_3$ )  $\delta$  (ppm) 1.5–1.7 (m, 5H), 1.8–1.9 (m, 1H), 2.83 (dd, 1H,  $J = 5.1, 9.0$  Hz), 3.62 (br s, 1H), 3.81 (br s, 1H), 7.70 (s, 4H), 8.06 (dd, 1H,  $J = 2.4, 3.6$  Hz), 8.13 (m, 1H);  $^{13}\text{C}$  NMR ( $\text{CDCl}_3$ )  $\delta$  (ppm) 29.6, 30.6, 31.8, 40.9, 44.7, 56.8, 63.2, 125.9 (q,  $J = 15$  Hz), 129.6 (d,  $J = 12.3$  Hz), 140.2 (d,  $J = 14.7$  Hz), 141.4 (d,  $J = 18.6$  Hz), 146.1 (d,  $J = 57.6$  Hz), 157.7, 160.8, 162.7.

Compound 5b-HCl was obtained as a yellow solid. Anal. ( $\text{C}_{18}\text{H}_{17}\text{ClF}_4\text{N}_2\cdot\text{H}_2\text{O}$ ) C, H, N.

**2'-Fluoro-3'-[4-(cyanophenyl)deschloroepibatidine (5c) Hydrochloride.** Data for 5c:  $^1\text{H}$  NMR ( $\text{CDCl}_3$ )  $\delta$  (ppm) 1.5–1.7 (m, 5H), 1.8–1.9 (m, 1H), 2.84 (dd, 1H,  $J = 5.1, 9.0$  Hz), 3.61 (br s, 1H), 3.82 (m, 1H), 7.6–7.8 (m, 4H), 8.09 (dd, 1H,  $J = 2.4, 6.6$  Hz), 8.14 (m, 1H);  $^{13}\text{C}$  NMR ( $\text{CDCl}_3$ )  $\delta$  (ppm) 29.6, 30.7, 31.9, 40.9, 44.6, 56.8, 63.2, 112.3, 118.9, 121.5 (d,  $J = 112.2$  Hz), 129.9 (d,  $J = 13.2$  Hz), 132.7, 139.3, 140.1, 141.6, 146.5 (d,  $J = 57.9$  Hz), 157.5, 160.7.

Compound 5c-HCl was obtained as a yellow solid. Anal. ( $\text{C}_{18}\text{H}_{17}\text{ClFN}_3\cdot 0.5\text{H}_2\text{O}$ ) C, H, N.

**2'-Fluoro-3'-[4-(methylsulfonyl)phenyl]deschloroepibatidine (5d) Hydrochloride.** Compound 11 (312 mg, 0.7 mmol) was dissolved in anhydrous  $\text{CH}_2\text{Cl}_2$  (3 mL) and cooled in an ice–water bath. TFA (3 mL) was added in 30 min. After being stirred at room temperature for 1 h, the mixture was poured into a cold solution of  $\text{NH}_4\text{OH}$  in water (1:1). The mixture was then extracted with  $\text{CH}_2\text{Cl}_2$ . The organic phase was washed with brine, dried ( $\text{Na}_2\text{SO}_4$ ), and evaporated to dryness. Flash chromatography on a silica gel column with  $\text{CH}_2\text{Cl}_2$ –MeOH gave 242 mg (99%) of the free base 5d as a clear oil:  $^1\text{H}$  NMR ( $\text{CDCl}_3$ )  $\delta$  (ppm) 1.5–1.7 (m, 5H), 1.8–1.9 (m, 1H),

2.87 (dd, 1H,  $J = 5.1, 9.0$  Hz), 3.11 (s, 3H), 3.65 (br s, 1H), 3.84 (m, 1H), 7.7–7.8 (m, 2H), 8.0–8.05 (m, 2H), 8.09 (dd, 1H,  $J = 2.4, 3.6$  Hz), 8.15 (m, 1H);  $^{13}\text{C}$  NMR ( $\text{CDCl}_3$ )  $\delta$  (ppm) 29.6, 30.5, 31.7, 40.8, 44.6, 44.9, 56.8, 63.2, 121.6 (d,  $J = 112.5$  Hz), 128.0, 130.2 (d,  $J = 12.3$  Hz), 140.3 (d,  $J = 14.7$  Hz), 141.3 (d,  $J = 18.6$  Hz), 146.6 (d,  $J = 57.6$  Hz), 157.6, 160.8.

The free base 5d (242 mg, 0.7 mmol) was dissolved in MeOH (7 mL) at room temperature. HCl (1 M in ether, 7 mL) was added with a syringe pump over 50 min at room temperature. After the mixture was stirred for 30 min, the solvent was removed. The residue was recrystallized from MeOH–ether to give 5d-HCl as a yellow solid. Anal. ( $\text{C}_{18}\text{H}_{20}\text{ClFN}_2\text{O}_2\text{S}\cdot 0.75\text{H}_2\text{O}$ ) C, H, N.

**2'-Fluoro-3'-[4-(aminosulfonyl)phenyl]deschloroepibatidine (5e) Hydrochloride.** A solution of 12 (245 mg, 0.55 mmol) in  $\text{CH}_2\text{Cl}_2$  (3 mL) and TFA (1 mL) was stirred at room temperature for 2 h. The solvent was removed under reduced pressure, and the residual was treated with a 20 mL solution of  $\text{NH}_4\text{OH}$ – $\text{H}_2\text{O}$  (3:1). The organic product was extracted with  $\text{CHCl}_3$  (3  $\times$  30 mL), dried over anhydrous sodium sulfate, filtered through Celite, and concentrated in vacuo. Purification of the residual by flash chromatography through an ISCO column provided 159 mg (84%) of 5e as a colorless oil:  $^1\text{H}$  NMR ( $\text{CD}_3\text{OD}$ )  $\delta$  (ppm) 1.48–1.80 (m, 5H), 2.02–2.09 (dd,  $J = 9.1, 12.3$  Hz, 1H), 3.02–3.07 (dd,  $J = 4.8, 8.9$  Hz, 1H), 3.67 (s, 1H), 3.76 (s, 1H), 7.78 (dd,  $J = 1.5, 8.5$  Hz, 2H), 7.91 (dd,  $J = 8.6, 1.9$  Hz, 2H), 8.06 (dd,  $J = 2.4, 9.5$  Hz, 1H), 8.14 (s, 1H);  $^{13}\text{C}$  NMR ( $\text{CD}_3\text{OD}$ )  $\delta$  (ppm) 29.9, 31.8, 41.0, 45.7, 57.9, 63.6, 104.6, 123.7 ( $J_{\text{CF}} = 28.2$  Hz), 127.5, 130.6, 130.6, 137.4 ( $J_{\text{CF}} = 4.6$  Hz), 141.5 ( $J_{\text{CF}} = 3.1$  Hz), 145.1, 146.7 ( $J_{\text{CF}} = 14.6$  Hz), 153.0, 157.6; MS (ESI)  $m/z$  348.1 (M + H) $^+$ .

The free base 5e was converted to 5e-HCl using HCl in diethyl ether: mp 205–208  $^\circ\text{C}$ ;  $^1\text{H}$  NMR (methanol- $d_4$ )  $\delta$  (ppm) 1.87–2.19 (m, 5H), 2.45–2.53 (dd,  $J = 9.6, 13.4$  Hz, 1H), 3.51–3.56 (dd,  $J = 4.8, 8.9$  Hz, 1H), 4.33 (s, 1H), 4.55 (s, 1H), 7.81 (dd,  $J = 1.5, 8.5$  Hz, 2H), 8.01 (dd,  $J = 1.8, 6.8$  Hz, 2H), 8.09 (dd,  $J = 2.4, 9.1$  Hz, 1H), 8.22 (s, 1H);  $^{13}\text{C}$  NMR (methanol- $d_4$ )  $\delta$  (ppm) 27.0, 29.1, 37.8, 43.4, 60.4, 64.3, 103.0, 123.2, 127.6, 130.7, 130.8, 137.6, 138.7, 141.6, 145.1, 146.7 ( $J_{\text{CF}} = 14.0$  Hz), 159.0, 162.2; MS (ESI)  $m/z$  348.1 [(M - HCl)] $^+$ , M =  $\text{C}_{16}\text{H}_{18}\text{FN}_3\text{O}_2\text{S}$ . Anal. ( $\text{C}_{17}\text{H}_{18}\text{ClFN}_3\text{O}_2\text{S}\cdot\text{H}_2\text{O}$ ) C, H, N.

**2'-Fluoro-3'-[4-[(trifluoromethyl)sulfonyl]phenyl]deschloroepibatidine (5f) Hydrochloride.** A solution of 16 (308 mg, 0.62 mmol) in  $\text{CH}_2\text{Cl}_2$  (3 mL) and TFA (1 mL) was stirred at room temperature for 2 h. The solvent was removed under reduced pressure, and the residual was treated with a 20 mL solution of  $\text{NH}_4\text{OH}$ – $\text{H}_2\text{O}$  (3:1). The organic product was extracted with  $\text{CHCl}_3$  (3  $\times$  30 mL), dried over anhydrous sodium sulfate, filtered through Celite, and concentrated in vacuo. Purification of the residual by flash chromatography through an ISCO column provided 202 mg (82%) of 5f as a colorless oil:  $^1\text{H}$  NMR ( $\text{CDCl}_3$ )  $\delta$  (ppm) 1.55–1.69 (m, 7H), 1.93–2.05 (dd,  $J = 9.0, 12.4$  Hz, 1H), 2.83–2.87 (dd,  $J = 4.8, 8.9$  Hz, 1H), 3.61 (s, 1H), 3.84 (s, 1H), 7.88 (dd,  $J = 1.4, 8.5$  Hz, 2H) 8.11–8.19 (m, 4H);  $^{13}\text{C}$  NMR ( $\text{CDCl}_3$ )  $\delta$  (ppm) 30.4, 31.56, 40.7, 44.3, 56.4, 62.9, 117.6, 120.4 ( $J_{\text{CF}} = 28.2$  Hz), 122.0, 130.2, 130.3, 131.0, 140.0 ( $J_{\text{CF}} = 3.4$  Hz), 141.5 ( $J_{\text{CF}} = 4.7$  Hz), 143.0 ( $J_{\text{CF}} = 5.6$  Hz), 146.8 ( $J_{\text{CF}} = 14.7$  Hz), 157.2, 160.3; MS (ESI)  $m/z$  401.2 (M + H) $^+$ .

The free base 5f was converted to 5f-HCl using HCl in diethyl ether: mp 144–148  $^\circ\text{C}$ ;  $^1\text{H}$  NMR (methanol- $d_4$ )  $\delta$  (ppm) 1.85–2.22 (m, 5H), 2.47–2.54 (dd,  $J = 9.6, 13.4$  Hz, 1H), 3.53–3.58 (dd,  $J = 4.8, 8.9$  Hz, 1H), 4.35 (s, 1H), 4.61 (s, 1H), 8.07 (dd,  $J = 1.4, 8.6$  Hz, 2H) 8.16 (dd,  $J = 2.4, 9.3$  Hz, 1H), 8.21 (d,  $J = 8.4$  Hz, 1H), 8.29 (s, 1H);  $^{13}\text{C}$  NMR (methanol- $d_4$ )  $\delta$  (ppm) 26.8, 28.9, 37.6, 43.3, 60.5, 64.3, 119.1, 122.2 ( $J_{\text{CF}} = 28.2$  Hz), 123.4, 132.0, 132.3, 137.5, 141.8, 143.9 ( $J_{\text{CF}} = 5.2$  Hz), 147.9 ( $J_{\text{CF}} = 14.8$  Hz), 158.9, 162.1; MS (ESI)  $m/z$  401.0 [(M - HCl)] $^+$ , M =  $\text{C}_{18}\text{H}_{16}\text{F}_4\text{N}_2\text{O}_2\text{S}$ . Anal. ( $\text{C}_{18}\text{H}_{16}\text{ClF}_4\text{N}_2\text{O}_2\text{S}\cdot\text{H}_2\text{O}$ ) C, H, N.

**2'-Fluoro-3'-[4-(carbamoyl)phenyl]deschloroepibatidine (5g) Hydrochloride.** A solution of 7 (178 mg, 0.66 mmol), 4-carbamoylphenylboronic acid (130 mg, 0.79 mmol), Pd( $\text{PPh}_3$ )<sub>4</sub> (38 mg, 5 mol %), and  $\text{K}_2\text{CO}_3$  (182 mg, 1.31 mmol) in 1,4-dioxane (5 mL) and  $\text{H}_2\text{O}$  (0.8 mL) in a sealed tube was degassed through bubbling  $\text{N}_2$  for 20 min and then heated at 100  $^\circ\text{C}$  for 20 h. After the

solution was cooled to room temperature, the solvent was removed in vacuo, and the residue was redissolved in EtOAc. Water (20 mL) was added and the organic product extracted with EtOAc (3 × 30 mL). The combined organic layers were dried (MgSO<sub>4</sub>), filtered through Celite, and concentrated in vacuo. The crude residue was purified on silica gel (CHCl<sub>3</sub>–MeOH) by flash chromatography to provide 160 mg (78% yield) of **5g** as a colorless oil: <sup>1</sup>H NMR (CDCl<sub>3</sub>) δ 1.53–1.72 (m, 5H), 1.91–1.98 (m, 3H), 2.82–2.86 (m, 1H), 3.61 (s, 1H), 3.80 (s, 1H), 6.58 (br s, 2H), 7.62–7.65 (m, 2H), 7.89–7.92 (m, 2H), 8.01 (dd, *J* = 2.4, 9.6 Hz, 1H), 8.10 (s, 1H); <sup>13</sup>C NMR (CDCl<sub>3</sub>) δ 30.2, 40.5, 44.4, 56.4, 62.8, 122.2, 127.1, 129.0, 133.1, 137.8, 139.8, 140.8, 145.6, 160.5, 169.1; MS (ESI) *m/z* 312.6 (M + H)<sup>+</sup>.

A solution of **5g** in chloroform in a vial was treated with a solution of HCl in diethyl ether. The excess solvent was removed in vacuo to give **5g**·HCl: mp 202–206 °C; <sup>1</sup>H NMR (CD<sub>3</sub>OD) δ 1.91–2.20 (m, 5H), 2.46–2.54 (dd, *J* = 3.8, 9.6 Hz, 1H), 3.51–3.56 (m, 1H), 4.35 (d, *J* = 3.5 Hz, 1H), 4.60 (d, *J* = 2.5 Hz, 1H), 7.77–7.74 (m, 2H), 7.99–8.02 (m, 2H), 8.10 (dd, *J* = 2.4, 9.2 Hz, 1H), 8.20 (s, 1H); <sup>13</sup>C NMR (CD<sub>3</sub>OD) δ 26.8, 28.9, 37.6, 43.3, 60.5, 64.3, 123.8, 129.1, 130.2, 135.0, 137.2, 138.3, 141.4, 146.4, 159.1, 162.3, 171.6; MS (ESI) *m/z* 312.4 (M + H)<sup>+</sup>. Anal. (C<sub>18</sub>H<sub>19</sub>ClFN<sub>3</sub>O·1.75H<sub>2</sub>O): C, H, N.

**7-(tert-Butoxycarbonyl)-2-exo-[2'-fluoro-3'-bromo-5'-pyridinyl]-7-azabicyclo[2.2.1]heptane (8)**. A solution of **7** (447 mg, 1.65 mmol) in CH<sub>2</sub>Cl<sub>2</sub> (15 mL) and Et<sub>3</sub>N (350 μL) was treated with (Boc)<sub>2</sub>O (540 mg, 2.47 mmol) and stirred overnight. The reaction mixture was then diluted with an additional CH<sub>2</sub>Cl<sub>2</sub> (20 mL) and washed with brine. The organic phase was dried over anhydrous Na<sub>2</sub>SO<sub>4</sub> and concentrated in vacuo. The resultant residue was purified by flash chromatography, and the title compound was isolated as a yellow oil (591 mg, 97%): <sup>1</sup>H NMR (CDCl<sub>3</sub>) δ (ppm) 7.8–8.0 (2H, m), 4.33 (br s, 1H), 4.11 (br s, 1H), 2.83 (dd, 1H, *J* = 4.8, 9.0 Hz), 1.96 (dd, 1H, *J* = 9.0, 12.3 Hz), 1.4–1.8 (5H, m), 1.39 (9H, s); <sup>13</sup>C NMR (CDCl<sub>3</sub>) δ (ppm) 160.2, 157.1, 144.9 (d, *J* = 21.9 Hz), 142.7 (d, *J* = 6.9 Hz), 141.2 (d, *J* = 19.8 Hz), 62.2, 56.3, 44.8, 40.8, 30.0, 29.1, 28.6.

#### General Procedure for the Synthesis of Compounds 9–11.

Compound **8** (0.7 mmol) was cross-coupled with the respective boronic acid (1.4 mmol), [4-(trifluoromethyl)phenyl-, 4-cyanophenyl-, or 4-(methylsulfonyl)phenyl]boronic acid] in the presence of Pd(OAc)<sub>2</sub> (0.07 mmol), tris(*o*-tolyl)phosphine (0.14 mmol), and Na<sub>2</sub>CO<sub>3</sub> (1.7 mmol) mixed in DME (2 mL) and H<sub>2</sub>O (0.5 mL). The mixture was purged with argon, sealed, and heated in an 85 °C oil bath overnight. After cooling, the mixture was filtered through Celite and washed with EtOAc. The organic phase was washed with brine, dried (Na<sub>2</sub>SO<sub>4</sub>), and concentrated in vacuo. The residue was purified by flash chromatography on a silica gel column using EtOAc–hexanes as the eluent.

**Data for 7-(tert-butoxycarbonyl)-2-exo-[2'-fluoro-3'-[4-(trifluoromethyl)phenyl]-5'-pyridinyl]-7-azabicyclo[2.2.1]heptane (9)**: <sup>1</sup>H NMR (CDCl<sub>3</sub>) δ (ppm) 1.43 (s, 9H), 1.5–1.9 (m, 5H), 2.02 (m, 1H), 2.98 (dd, 1H, *J* = 4.8, 9.0 Hz), 4.25 (br s, 1H), 4.41 (br s, 1H), 7.70 (s, 4H), 7.91 (dd, 1H, *J* = 2.4, 6.3 Hz), 8.10 (m, 1H); <sup>13</sup>C NMR (CDCl<sub>3</sub>) δ (ppm) 28.3, 28.9, 29.7, 40.7, 44.8, 56.1, 62.1, 80.0, 125.6 (q, *J* = 15 Hz), 129.3 (d, *J* = 12.6 Hz), 137.9 (d, *J* = 18.6 Hz), 139.4 (d, *J* = 15.3 Hz), 140.0 (d, *J* = 19.5 Hz), 145.7 (d, *J* = 58.2 Hz), 155.0, 157.5, 160.7.

**Data for 7-(tert-butoxycarbonyl)-2-exo-[2'-fluoro-3'-(4-cyanophenyl)-5'-pyridinyl]-7-azabicyclo[2.2.1]heptane (10)**: <sup>1</sup>H NMR (CDCl<sub>3</sub>) δ (ppm) 1.43 (s, 9H), 1.5–1.9 (m, 5H), 2.02 (m, 1H), 2.99 (dd, 1H, *J* = 4.8, 9.0 Hz), 4.25 (br s, 1H), 4.41 (br s, 1H), 7.6–7.8 (m, 4H), 7.92 (dd, 1H, *J* = 2.4, 9.6 Hz), 8.12 (m, 1H); <sup>13</sup>C NMR (CDCl<sub>3</sub>) δ (ppm) 28.6, 29.2, 30.0, 41.0, 45.0, 56.3, 62.3, 80.3, 112.4, 116.7, 118.8, 121.7 (d, *J* = 112.5 Hz), 129.8 (d, *J* = 12.9 Hz), 132.7, 139.1, 139.5, 140.4, 146.5 (d, *J* = 58.2 Hz), 155.3, 157.6, 160.8.

**Data for 7-(tert-butoxycarbonyl)-2-exo-[2'-fluoro-3'-(4-(methylsulfonyl)phenyl)-5'-pyridinyl]-7-azabicyclo[2.2.1]heptane (11)**: <sup>1</sup>H NMR (CDCl<sub>3</sub>) δ (ppm) 1.58 (s, 9H), 1.5–1.9 (m, 5H), 2.02 (m, 1H), 3.00 (dd, 1H, *J* = 4.8, 9.0 Hz), 3.12 (s, 3H), 4.25 (br s, 1H), 4.41 (br s, 1H), 7.7–7.8 (m, 2H), 7.93 (dd, 1H, *J* = 2.4, 9.6 Hz), 8.0–8.1 (m, 2H), 8.13 (m, 1H); <sup>13</sup>C NMR (CDCl<sub>3</sub>) δ (ppm) 28.6, 29.2,

30.0, 41.0, 44.9, 45.0, 56.4, 62.4, 80.3, 116.4, 121.8 (d, *J* = 58.2 Hz), 128.1, 130.1 (d, *J* = 13.2 Hz), 139.7, 140.0, 140.4, 146.5 (d, *J* = 58.8 Hz), 155.4, 157.7, 160.9.

**7-(tert-Butoxycarbonyl)-2-exo-[2'-fluoro-3'-(4-sulfamoylphenyl)-5'-pyridinyl]-7-azabicyclo[2.2.1]heptane (12)**. A solution of **8** (488 mg, 1.32 mmol), 4-boronobenzenesulfonamide (318 mg, 1.58 mmol), PdCl<sub>2</sub>(dppf) (48 mg, 0.066 mmol), and K<sub>2</sub>CO<sub>3</sub> (547 mg, 3.96 mmol) in 1,4-dioxane (3 mL) and H<sub>2</sub>O (1 mL) was placed in a microwave vial and degassed through bubbling nitrogen for 20 min. The reaction mixture was then irradiated in a CEM Corp. microwave reactor for 20 min at 140 °C. After being cooled to room temperature, the mixture was diluted with a 10 mL CHCl<sub>3</sub>–MeOH (10:1) solution and decanted into a 10 mL aqueous solution of NaHCO<sub>3</sub>. The organic product was extracted with chloroform (3 × 20 mL), and the combined organic layers were dried (Na<sub>2</sub>SO<sub>4</sub>), filtered through Celite, and concentrated in vacuo. The resultant residue was purified by flash chromatography through an ISCO column to furnish 245 mg (41%) of **12** as a foamy solid: <sup>1</sup>H NMR (CDCl<sub>3</sub>) δ (ppm) 1.41 (s, 9H), 1.53–1.66 (m, 2H), 1.81–1.93 (m, 3H), 1.98–2.09 (dd, *J* = 9.0, 12.4 Hz, 1H), 2.95–3.00 (dd, *J* = 4.8, 8.9 Hz, 1H), 4.24 (s, 1H), 4.40 (s, 1H), 5.47 (s, 2H), 7.67 (dd, *J* = 1.4, 8.5 Hz, 2H), 7.91 (dd, *J* = 9.6, 2.4 Hz, 1H), 7.98 (dd, *J* = 1.9, 8.6 Hz, 2H), 8.10 (s, 1H); <sup>13</sup>C NMR (CDCl<sub>3</sub>) δ (ppm) 28.3 (3C), 28.8, 29.6, 40.4, 44.7, 56.0, 61.9, 80.1, 121.4 (*J*<sub>CF</sub> = 28.2 Hz), 126.6, 129.4, 129.4, 138.2 (*J*<sub>CF</sub> = 5.2 Hz), 139.5 (*J*<sub>CF</sub> = 3.7 Hz), 140.0 (*J*<sub>CF</sub> = 4.8 Hz), 142.2, 145.6, (*J*<sub>CF</sub> = 15.0 Hz), 155.0, 157.3, 160.5.

**7-(tert-Butoxycarbonyl)-2-exo-[2'-fluoro-3'-(4,4,5,5-tetramethyl-1,3,2-dioxaborolan-2-yl)-5'-pyridinyl]-7-azabicyclo[2.2.1]heptane (13)**. In a microwave vial were placed **8** (214 mg, 0.578 mmol, 1.0 equiv), bis(pinacolato)diboron (176 mg, 0.694 mmol, 1.2 equiv), KOAc (170 mg, 1.73 mmol, 3.0 equiv), PdCl<sub>2</sub>(dppf) (21 mg, 0.0289 mmol, 5 mol %), and anhydrous 1,4-dioxane (3 mL). The mixture was degassed through bubbling nitrogen for 20 min followed by irradiation in a microwave at 140 °C for 20 min. After being cooled to room temperature, the mixture was diluted with EtOAc, filtered through a plug of Celite and anhydrous Na<sub>2</sub>SO<sub>4</sub>, and concentrated in vacuo. The resultant residue was purified by flash chromatography through a Teledyne ISCO column (EtOAc–hexanes) to provide 589 mg (94%) of **13** as a colorless oil: <sup>1</sup>H NMR (CDCl<sub>3</sub>) δ (ppm) 1.26 (s, 12H), 1.44 (s, 9H), 1.60–1.53 (m, 2H), 1.75–1.92 (m, 3H), 1.96–2.03 (dd, *J* = 9.0, 12.4 Hz, 1H), 2.87–2.92 (dd, *J* = 4.8, 8.9 Hz, 1H), 4.19 (s, 1H), 4.40 (s, 1H), 8.07 (dd, *J* = 8.4, 2.4 Hz, 1H), 8.17 (d, *J* = 2.7 Hz, 1H); <sup>13</sup>C NMR (CDCl<sub>3</sub>) δ (ppm) 24.8, 28.3 (3C), 28.8, 29.8, 40.2, 44.9, 61.8, 79.7, 84.3, 138.2 (*J*<sub>CF</sub> = 5.0 Hz), 146.8, 149.2 (*J*<sub>CF</sub> = 15.0 Hz), 154.9, 164.2, 167.4; MS (ESI) *m/z* 419.7 (M + H)<sup>+</sup>.

**1-Bromo-4-[(trifluoromethyl)sulfonyl]benzene (15)**. A stirred ice-cold solution of 4-bromophenyl trifluoromethyl sulfide (**14**) (1.5 g, 5.83 mmol) in CH<sub>2</sub>Cl<sub>2</sub> (40 mL) was treated with mCPBA (5.03 g, 29.2 mmol), and the reaction mixture was allowed to warm to room temperature. Stirring was continued overnight, after which the reaction mixture was diluted with additional CH<sub>2</sub>Cl<sub>2</sub> (60 mL) and washed sequentially with an aqueous saturated NaHCO<sub>3</sub> solution (50 mL) and brine (50 mL). The organic layer was dried over anhydrous MgSO<sub>4</sub>, filtered through Celite, and concentrated in vacuo to provide 1.12 g (67%) of **15** as a white crystalline solid that was used without further purification.

**7-(tert-Butoxycarbonyl)-2-exo-[2'-fluoro-3'-[4-[(trifluoromethyl)sulfonyl]phenyl]-5'-pyridinyl]-7-azabicyclo[2.2.1]heptane (16)**. A solution of the boronic ester **13** (480 mg, 1.15 mmol), **15** (431 mg, 1.49 mmol), Pd(PPh<sub>3</sub>)<sub>4</sub> (133 mg, 0.115 mmol), and K<sub>2</sub>CO<sub>3</sub> (462 mg, 3.34 mmol) in DME–EtOH–H<sub>2</sub>O (3.2 mL/0.8 mL/1 mL) was placed in a microwave vial and degassed through bubbling nitrogen for 20 min. The mixture was irradiated in a CEM Corp. microwave reactor for 20 min at 140 °C. After the mixture was cooled to room temperature, the solvent was removed under reduced pressure, the residue was redissolved in CH<sub>2</sub>Cl<sub>2</sub> (10 mL), and H<sub>2</sub>O (10 mL) was added. The organic product was extracted with CH<sub>2</sub>Cl<sub>2</sub> (3 × 20 mL), the combined organic layers were dried (Na<sub>2</sub>SO<sub>4</sub>) and filtered through Celite, and the solvent was removed in vacuo. The resultant residue was purified by flash chromatography through a Teledyne ISCO



column to furnish 408 mg (71%) of **16** as a colorless oil:  $^1\text{H}$  NMR ( $\text{CDCl}_3$ )  $\delta$  (ppm) 1.43 (s, 9H), 1.55–1.68 (m, 2H), 1.82–1.92 (m, 3H), 2.05–2.12 (dd,  $J = 9.0, 12.4$  Hz, 1H), 2.98–3.03 (dd,  $J = 4.8, 8.9$  Hz, 1H), 4.25 (s, 1H), 4.42 (s, 1H), 7.87 (d,  $J = 8.3$  Hz, 2H), 7.98 (dd,  $J = 9.6, 2.6$  Hz, 1H), 8.11 (d,  $J = 8.4$  Hz, 2H), 8.16 (s, 1H);  $^{13}\text{C}$  NMR ( $\text{CDCl}_3$ )  $\delta$  (ppm) 28.3 (3C), 28.8, 29.6, 40.7, 44.7, 56.0, 61.9, 80.0, 117.6, 120.6 ( $J_{\text{CF}} = 28.3$  Hz), 121.9, 130.2, 130.2, 130.9, 139.4 ( $J_{\text{CF}} = 3.3$  Hz), 140.2 ( $J_{\text{CF}} = 4.9$  Hz), 142.7 ( $J_{\text{CF}} = 5.6$  Hz), 146.8 ( $J_{\text{CF}} = 15.0$  Hz), 154.9, 157.3, 160.5.

**$^3\text{H}$ Epibatidine Binding Assay.** Adult male rat cerebral cortices (Pel-Freez Biologicals, Rogers, AK) were homogenized in 39 volumes of ice-cold 50 mM Tris buffer (pH 7.4 at 4 °C) containing 120 mM NaCl, 5 mM KCl, 2 mM  $\text{CaCl}_2$ , and 1 mM  $\text{MgCl}_2$  and sedimented at 37000g for 10 min at 4 °C. The supernatant was discarded, the pellet resuspended in the original volume of buffer, and the wash procedure repeated two more times. After the last centrifugation, the pellet was resuspended in 1/10 its original homogenization volume and stored at –80 °C until needed. In a final volume of 0.5 mL, each assay tube contained 3 mg wet weight of male rat cerebral cortex homogenate (added last), 0.5 nM  $^3\text{H}$ epibatidine (NEN Life Science Products, Wilmington, DE), and 1 of 10–12 different concentrations of test compound dissolved in buffer (pH 7.4 at room temperature) containing 10% DMSO, resulting in a final DMSO concentration of 1%. Total and nonspecific bindings were determined in the presence of vehicle and 300  $\mu\text{M}$  (–)nicotine, respectively. After a 4 h incubation period at room temperature, the samples were vacuum-filtered over GF/B filter papers presoaked in 0.03% poly(ethylenimine) using a Brandel 48-well harvester and washed with 6 mL of ice-cold buffer. The amount of radioactivity trapped on the filter was determined by standard liquid scintillation techniques in a TriCarb 2200 scintillation counter (Packard Instruments, Meriden, CT) at approximately 50% efficiency. The binding data were fit using the nonlinear regression analysis routines in Prism (Graphpad, San Diego, CA). The  $K_i$  values for the test compounds were calculated from their respective  $\text{IC}_{50}$  values using the Cheng–Prusoff equation.

**$^{125}\text{I}$ Iodo-MLA Binding Assay.** Adult male rat cerebral cortices (Pel-Freez Biologicals) were homogenized (polytron) in 39 volumes of ice-cold 50 mM Tris buffer (assay buffer; pH 7.4 at 4 °C) containing 120 mM NaCl, 5 mM KCl, 2 mM  $\text{CaCl}_2$ , and 1 mM  $\text{MgCl}_2$ . The homogenate was centrifuged at 35000g for 10 min at 4 °C and the supernatant discarded. The pellet was resuspended in the original volume of buffer and the wash procedure repeated two more times. After the last centrifugation step, the pellet was resuspended in 1/10 the original homogenization volume and stored at –80 °C until needed. Triplicate samples were run in 1.4 mL polypropylene tubes (Matrix Technologies Corp., Hudson, NH). Briefly, in a final volume of 0.5 mL, each assay sample contained 3 mg wet weight of rat cerebral cortex (added last), 40–50 pM  $^{125}\text{I}$ iodo-MLA, and a 50 nM final concentration of test compound dissolved in buffer containing 10% DMSO, giving a final DMSO concentration of 1%. Total and nonspecific binding were determined in the presence of vehicle and 300  $\mu\text{M}$  (–)nicotine, respectively. After a 2 h incubation period on ice, the samples were vacuum-filtered using a Multimate 96-well harvester (Packard Instruments) onto GF/B filters presoaked for at least 30 min in assay buffer containing 0.15% bovine serum albumin. Each well was then washed with approximately 3.0 mL of ice-cold buffer. The filter plates were dried, and 30  $\mu\text{L}$  of Microscint20 (Packard) was added to each well. The amount of radioligand remaining on each filter was determined using a TopCount 12-detector (Packard) microplate scintillation counter at approximately 70% efficiency.

**Tail-Flick Test.** Antinociception was assessed by the tail-flick method of D'Amour and Smith.<sup>34</sup> A control response (2–4 s) was determined for each mouse before treatment, and a test latency was determined after drug administration. To minimize tissue damage, a maximum latency of 10 s was imposed. Antinociceptive response was calculated as the maximum possible effect (MPE; %), where  $\text{MPE} (\%) = [(\text{test} - \text{control}) / (10 - \text{control})] \times 100$ . Groups of eight to twelve animals were used for each dose and for each treatment. The mice were tested 5 min after subcutaneous (sc) injections of epibatidine analogues for the dose–response evaluation. Eight to twelve mice were

treated per dose, and a minimum of four doses were performed for dose–response curve determination.

**Hot-Plate Test.** Mice were placed into a 10 cm wide glass cylinder on a hot plate (Thermojust Apparatus) maintained at 55 °C. Two control latencies at least 10 min apart were determined for each mouse. The normal latency (reaction time) was 8–12 s. Antinociceptive response was calculated as the MPE, where  $\text{MPE} (\%) = [(\text{test} - \text{control}) / (40 - \text{control})] \times 100$ . The reaction time was scored when the animal jumped or licked its paws. Eight mice per dose were given sc injections of epibatidine analogues and tested 5 min thereafter to establish a dose–response curve.

**Locomotor Activity.** Mice were placed into individual Omnitech photocell activity cages (28  $\times$  16.5 cm) 5 min after sc administration of either 0.9% saline or epibatidine analogues. Interruptions of the photocell beams (two banks of eight cells each) were then recorded for the next 10 min. Data are expressed as the number of photocell interruptions.

**Body Temperature.** Rectal temperature was measured by a thermistor probe (inserted 24 mm) and digital thermometer (Yellow Springs Instrument Co., Yellow Springs, OH). Readings were taken just before and 30 min after the sc injection of either saline or epibatidine analogues. The difference in rectal temperature before and after treatment was calculated for each mouse. The ambient temperature of the laboratory varied from 21 to 24 °C from day to day.

**Electrophysiology.** *Xenopus laevis* oocytes were surgically obtained, and follicle cells were removed by treatment with collagenase B for 2 h at room temperature. cRNA encoding the rat  $\alpha_3$ ,  $\alpha_4$ ,  $\alpha_7$ ,  $\beta_2$ , and  $\beta_4$  neuronal nAChR subunits was synthesized using mMessage mMachine kits (Ambion). Oocytes were injected with 10–40 ng of cRNA in 25–50 nL of water and incubated at 19 °C in modified Barth's saline (88 mM NaCl, 1 mM KCl, 2.4 mM  $\text{NaHCO}_3$ , 0.3 mM  $\text{Ca}(\text{NO}_3)_2$ , 0.41 mM  $\text{CaCl}_2$ , 0.82 mM  $\text{MgSO}_4$ , 150  $\mu\text{g}/\text{mL}$  ceftazidime, 15 mM HEPES, pH 7.6). For  $\alpha_4\beta_2$  and  $\alpha_3\beta_4$  receptors, cRNA transcripts encoding each subunit were injected into oocytes at a molar ratio of 1:1. Agonist-induced current responses were measured 2–6 days after cRNA injection using a two-electrode voltage clamp in an automated parallel electrophysiology system (OpusExpress 6000A, Molecular Devices). Micropipets were filled with 3 M KCl and had resistances of 0.2–2.0 M $\Omega$ . For  $\alpha_4\beta_2$  and  $\alpha_3\beta_4$  receptors, current responses were recorded at a holding potential of –70 mV, filtered (4-pole, Bessel, low pass) at 20 Hz (–3db), and sampled at 100 Hz. For  $\alpha_7$  receptors, current responses were recorded at a holding potential of –40 mV (to minimize the contribution of  $\text{Ca}^{2+}$ -activated  $\text{Cl}^-$  channels), filtered (4-pole, Bessel, low pass) at 100 Hz (–3db), and sampled at 500 Hz. Current responses were captured and stored using OpusXpress 1.1 software (Molecular Devices). Oocytes were perfused at room temperature (20–25 °C) with ND96 (96 mM NaCl, 2 mM KCl, 1 mM  $\text{CaCl}_2$ , 1 mM  $\text{MgCl}_2$ , 5 mM HEPES, pH 7.5). Compounds, diluted in ND96, were applied for 15 s ( $\alpha_4\beta_2$  and  $\alpha_3\beta_4$ ) or 5 s ( $\alpha_7$ ) at a flow rate of 4 mL/min, with 3 min washes between applications. Agonist activity was assessed (Table 1) by comparing the current response to a 100  $\mu\text{M}$  concentration of each compound to the mean current response of three preceding applications of acetylcholine, applied at an  $\text{EC}_{20}$  concentration (20  $\mu\text{M}$  for  $\alpha_4\beta_2$ , 110  $\mu\text{M}$  for  $\alpha_3\beta_4$ ) or an  $\text{EC}_{50}$  concentration (300  $\mu\text{M}$  for  $\alpha_7$ ). The agonist activity of each compound is expressed as a percentage of the maximal response to acetylcholine. Antagonist activity was initially assessed (Table 1) by comparing the current response to an  $\text{EC}_{50}$  concentration of acetylcholine (70  $\mu\text{M}$  for  $\alpha_4\beta_2$ , 200  $\mu\text{M}$  for  $\alpha_3\beta_4$ , 300  $\mu\text{M}$  for  $\alpha_7$ ) in the presence of a 100  $\mu\text{M}$  concentration of each compound to the mean current response of three preceding applications of acetylcholine ( $\text{EC}_{50}$  concentration). The antagonist activity of some compounds was assessed in more detail (Table 2) by generating concentration–inhibition curves. Data were fit (Prism 5, Graphpad) to the equation  $I = I_{\text{max}} / [1 + (\text{IC}_{50}/X)^n]$ , where  $I$  is the current response at the agonist concentration ( $X$ ),  $I_{\text{max}}$  is the maximum current,  $\text{IC}_{50}$  is the ligand concentration producing half-maximal inhibition of the current response, and  $n$  is the Hill coefficient.

**Molecular Modeling.** Ligand–receptor docking simulations were performed using Tripos Sybyl-X (version 2.01) running on an eight-core Macintosh workstation. Ligand models were built using the Sybyl

fragment library and energy-minimized using the Tripos force field and Gasteiger–Marsili charges.

The receptor structure used for the docking studies was the X-ray crystallographic coordinates of a human  $\alpha 7$ -nicotinic receptor–mollusk (*L. stagnalis*) acetylcholine binding protein chimera complexed with epibatidine (PDB 3SQ6). The “A” and “B” subunits of 3SQ6 and the associated ligand (epibatidine) were selected for the calculations. AMBER7 FF99 (biopolymer) and Gasteiger–Marsili (ligand) charges were applied to the receptor–ligand complex in preparation for use in docking studies. The Surfex “protomol” was generated on the basis of the X-ray coordinates of the bound ligand with a threshold parameter of 0.5 and “bloat” value of 4.

The Surfex-Dock calculations were performed with default parameters plus options selected for full flexibility of both the ligand and the receptor ligand binding domain. Twenty poses for each ligand were examined, and on the basis of the Surfex “total score” (an estimated  $-\log(K_d)$ ), the optimal pose for each ligand was selected. A postdock minimization was performed for both the ligand and receptor, and a final score was calculated on the basis of this optimized docked structure.

## ■ ASSOCIATED CONTENT

### ■ Supporting Information

Elemental analysis data. This material is available free of charge via the Internet at <http://pubs.acs.org>.

## ■ AUTHOR INFORMATION

### Corresponding Author

\*Phone: (919) 541-6679. Fax: (919) 541-8868. E-mail: [fic@rti.org](mailto:fic@rti.org).

### Notes

The authors declare no competing financial interest.

## ■ ACKNOWLEDGMENTS

This research was supported by the National Institute on Drug Abuse (Grant DA12001).

## ■ ABBREVIATIONS USED

Ls-AChBP, *Lymnaea stagnalis* acetylcholine binding protein; NRT, nicotine replacement therapy; CDC, Centers for Disease Control; nAChR, nicotinic acetylcholine receptor; AChBP, acetylcholine binding protein; ICSS, intracranial self-stimulation; CPP, conditioned place preference; DD, drug discrimination; SA, self-administration; PdCl<sub>2</sub>(dppf), [1,1'-bis(diphenylphosphino)ferrocene]palladium(II) dichloride; MCPBA, *m*-chloroperoxybenzoic acid; MPE, maximum potential effect; DH $\beta$ E, dihydro- $\beta$ -erythroidine

## ■ REFERENCES

- (1) Centers for Disease Control and Prevention. Smoking & Tobacco Use Fact Sheet: Smoking Cessation (updated November 2011). [http://www.cdc.gov/tobacco/data\\_statistics/fact\\_sheets/cessation/quitting/index.htm](http://www.cdc.gov/tobacco/data_statistics/fact_sheets/cessation/quitting/index.htm) (accessed January 2012).
- (2) Dwoskin, L. P.; Smith, A. M.; Wooters, T. E.; Zhang, Z.; Crooks, P. A.; Bardo, M. T. Nicotinic receptor-based therapeutics and candidates for smoking cessation. *Biochem. Pharmacol.* **2009**, *78*, 732–743.
- (3) Fowler, C. D.; Arends, M. A.; Kenny, P. J. Subtypes of nicotinic acetylcholine receptors in nicotine reward, dependence, and withdrawal: evidence from genetically modified mice. *Behav. Pharmacol.* **2008**, *19*, 461–484.
- (4) Russo, P.; Cesario, A.; Rutella, S.; Veronesi, G.; Spaggiari, L.; Galetta, D.; Margaritora, S.; Granone, P.; Greenberg, D. S. Impact of genetic variability in nicotinic acetylcholine receptors on nicotine

addiction and smoking cessation treatment. *Curr. Med. Chem.* **2011**, *18*, 91–112.

(5) Joslyn, G.; Brush, G.; Robertson, M.; Smith, T. L.; Kalmijn, J.; Schuckit, M.; White, R. L. Chromosome 15q25.1 genetic markers associated with level of response to alcohol in humans. *Proc. Natl. Acad. Sci. U.S.A.* **2008**, *105*, 20368–20373.

(6) Saccone, N. L.; Wang, J. C.; Breslau, N.; Johnson, E. O.; Hatsukami, D.; Saccone, S. F.; Grucza, R. A.; Sun, L.; Duan, W.; Budde, J.; Culverhouse, R. C.; Fox, L.; Hinrichs, A. L.; Steinbach, J. H.; Wu, M.; Rice, J. P.; Goate, A. M.; Bierut, L. J. The CHRNA5-CHRNA3-CHRNA4-CHRNA6 nicotinic receptor subunit gene cluster affects risk for nicotine dependence in African-Americans and in European-Americans. *Cancer Res.* **2009**, *69*, 6848–6856.

(7) Wang, H. Y.; Lee, D. H.; D'Andrea, M. R.; Peterson, P. A.; Shank, R. P.; Reitz, A. B. Beta-amyloid(1–42) binds to alpha7 nicotinic acetylcholine receptor with high affinity. Implications for Alzheimer's disease pathology. *J. Biol. Chem.* **2000**, *275*, 5626–5632.

(8) Frahm, S.; Slimak, M. A.; Ferrarese, L.; Santos-Torres, J.; Antolin-Fontes, B.; Auer, S.; Filkin, S.; Pons, S.; Fontaine, J. F.; Tsetlin, V.; Maskos, U.; Ibanez-Tallon, I. Aversion to nicotine is regulated by the balanced activity of beta4 and alpha5 nicotinic receptor subunits in the medial habenula. *Neuron* **2011**, *70*, 522–535.

(9) Gallego, X.; Molas, S.; Amador-Arjona, A.; Marks, M. J.; Robles, N.; Murtra, P.; Armengol, L.; Fernandez-Montes, R. D.; Gratacos, M.; Pumarola, M.; Cabrera, R.; Maldonado, R.; Sabria, J.; Estivill, X.; Dierssen, M. Overexpression of the CHRNA5/A3/B4 genomic cluster in mice increases the sensitivity to nicotine and modifies its reinforcing effects. *Amino Acids* **2012**, DOI: 10.1007/s00726-011-1149-y.

(10) Toll, L.; Zaveri, N. T.; Polgar, W. E.; Jiang, F.; Khroyan, T. V.; Zhou, W.; Xie, X. S.; Stauber, G. B.; Costello, M. R.; Leslie, F. M. AT-1001: a high affinity and selective  $\alpha 3/\beta 4$  nicotinic acetylcholine receptor antagonist blocks nicotine self-administration in rats. *Neuropsychopharmacology* **2012**, *37*, 1367–1376.

(11) Chatterjee, S.; Steensland, P.; Simms, J. A.; Holgate, J.; Coe, J. W.; Hurst, R. S.; Shaffer, C. L.; Lowe, J. A.; Rollema, H.; Bartlett, S. E. Partial agonists of the  $\alpha 3\beta 4^*$  neuronal nicotinic acetylcholine receptor reduce ethanol consumption and seeking in rats. *Neuropsychopharmacology* **2011**, *36*, 603–615.

(12) Johnston, A. J.; Ascher, J.; Leadbetter, R.; Schmith, V. D.; Patel, D. K.; Durcan, M.; Bentley, B. Pharmacokinetic optimization of sustained-release bupropion for smoking cessation. *Drugs* **2002**, *62* (Suppl. 2), 11–24.

(13) Hesse, L. M.; Venkatakrishnan, K.; Court, M. H.; von Moltke, L. L.; Duan, S. X.; Shader, R. I.; Greenblatt, D. J. CYP2B6 mediates the in vitro hydroxylation of bupropion: potential drug interactions with other antidepressants. *Drug Metab. Dispos.* **2000**, *28*, 1176–1183.

(14) Carroll, F. I.; Ma, W.; Deng, L.; Navarro, H. A.; Damaj, M. I.; Martin, B. R. Synthesis, nicotinic acetylcholine receptor binding, and antinociceptive properties of 3'-(substituted phenyl)epibatidine analogues. Nicotinic partial agonists. *J. Nat. Prod.* **2010**, *73*, 306–312.

(15) Carroll, F. I.; Yokota, Y.; Ma, W.; Lee, J. R.; Brieady, L. E.; Burgess, J. P.; Navarro, H. A.; Damaj, M. I.; Martin, B. R. Synthesis, nicotinic acetylcholine receptor binding, and pharmacological properties of 3'-(substituted phenyl)deschloroepibatidine analogs. *Bioorg. Med. Chem.* **2008**, *16*, 746–754.

(16) Carroll, F. I.; Ma, W.; Yokota, Y.; Lee, J. R.; Brieady, L. E.; Navarro, H. A.; Damaj, M. I.; Martin, B. R. Synthesis, nicotinic acetylcholine receptor binding, and antinociceptive properties of 3'-substituted deschloroepibatidine analogues. Novel nicotinic antagonists. *J. Med. Chem.* **2005**, *48*, 1221–1228.

(17) Carroll, F. I.; Ware, R.; Brieady, L. E.; Navarro, H. A.; Damaj, M. I.; Martin, B. R. Synthesis, nicotinic acetylcholine receptor binding, and antinociceptive properties of 2'-fluoro-3'-(substituted phenyl)-deschloroepibatidine analogs. Novel nicotinic antagonist. *J. Med. Chem.* **2004**, *47*, 4588–4594.

(18) Carroll, F. I.; Lee, J. R.; Navarro, H. A.; Ma, W.; Brieady, L. E.; Abraham, P.; Damaj, M. I.; Martin, B. R. Synthesis, nicotinic acetylcholine receptor binding, and antinociceptive properties of 2-

exo-2-(2',3'-disubstituted 5'-pyridinyl)-7-azabicyclo[2.2.1]heptanes: epibatidine analogues. *J. Med. Chem.* **2002**, *45*, 4755–4761.

(19) Carroll, F. I.; Lee, J. R.; Navarro, H. A.; Brieady, L. E.; Abraham, P.; Damaj, M. I.; Martin, B. R. Synthesis, nicotinic acetylcholine receptor binding, and antinociceptive properties of 2-exo-2-(2'-substituted-3'-phenyl-5'-pyridinyl)-7-azabicyclo[2.2.1]-heptanes. Novel nicotinic antagonist. *J. Med. Chem.* **2001**, *44*, 4039–4041.

(20) Carroll, F. I.; Liang, F.; Navarro, H. A.; Brieady, L. E.; Abraham, P.; Damaj, M. I.; Martin, B. R. Synthesis, nicotinic acetylcholine receptor binding, and antinociceptive properties of 2-exo-2-(2'-substituted 5'-pyridinyl)-7-azabicyclo[2.2.1]heptanes. Epibatidine analogues. *J. Med. Chem.* **2001**, *44*, 2229–2237.

(21) Abdrakhmanova, G. R.; Damaj, M. I.; Carroll, F. I.; Martin, B. R. 2-Fluoro-3-(4-nitro-phenyl)deschloroepibatidine is a novel potent competitive antagonist of human neuronal  $\alpha 4\beta 2$  nAChRs. *Mol. Pharmacol.* **2006**, *69*, 1945–1952.

(22) Tobey, K. M.; Walentiny, D. M.; Wiley, J. L.; Carroll, F. I.; Damaj, M. I.; Azar, M. R.; Koob, G. F.; George, O.; Harris, L. S.; Vann, R. E. Effects of the specific  $\alpha 4\beta 2$  nAChR antagonist, 2-fluoro-3-(4-nitrophenyl)deschloroepibatidine, on nicotine reward-related behaviors. *Psychopharmacology (Berlin)* **2012**, DOI: 10.1007/s00213-012-2703-3.

(23) Li, S. X.; Huang, S.; Bren, N.; Noridomi, K.; Dellisanti, C. D.; Sine, S. M.; Chen, L. Ligand-binding domain of an alpha7-nicotinic receptor chimera and its complex with agonist. *Nat. Neurosci.* **2011**, *14*, 1253–1259.

(24) SYBYL-X 1.2; Tripos International: St. Louis, MO, 2012.

(25) Huang, Y.; Zhu, Z.; Xiao, Y.; Laruelle, M. Epibatidine analogues as selective ligands for the alpha(x)beta2-containing subtypes of nicotinic acetylcholine receptors. *Bioorg. Med. Chem. Lett.* **2005**, *15*, 4385–4388.

(26) Carroll, F. I. Epibatidine structure-activity relationships. *Bioorg. Med. Chem. Lett.* **2004**, *14*, 1889–1896.

(27) Hansch, C.; Leo, A. Electronic effects on organic reactions. In *Exploring QSAR: Fundamentals and Applications in Chemistry and Biology*; American Chemical Society: Washington, DC, 1995; p 7.

(28) Stokes, C.; Papke, J. K.; Horenstein, N. A.; Kem, W. R.; McCormack, T. J.; Papke, R. L. The structural basis for GTS-21 selectivity between human and rat nicotinic alpha7 receptors. *Mol. Pharmacol.* **2004**, *66*, 14–24.

(29) Coe, J. W.; Brooks, P. R.; Vetelino, M. G.; Wirtz, M. C.; Arnold, E. P.; Huang, J.; Sands, S. B.; Davis, T. I.; Lebel, L. A.; Fox, C. B.; Shrikhande, A.; Heym, J. H.; Schaeffer, E.; Rollema, H.; Lu, Y.; Mansbach, R. S.; Chambers, L. K.; Rovetti, C. C.; Schulz, D. W.; Tingley, F. D., 3rd; O'Neill, B. T. Varenicline: an  $\alpha 4\beta 2$  nicotinic receptor partial agonist for smoking cessation. *J. Med. Chem.* **2005**, *48*, 3474–3477.

(30) Mihalak, K. B.; Carroll, F. I.; Luetje, C. W. Varenicline is a partial agonist at alpha4beta2 and a full agonist at alpha7 neuronal nicotinic receptors. *Mol. Pharmacol.* **2006**, *70*, 801–805.

(31) Avalos, M.; Parker, M. J.; Maddox, F. N.; Carroll, F. I.; Luetje, C. W. Effects of pyridine ring substitutions on the affinity, efficacy, and subtype selectivity of the neuronal nicotinic receptor agonist epibatidine. *J. Pharmacol. Exp. Ther.* **2002**, *302*, 1246–1252.

(32) Jensen, A. A.; Frolund, B.; Liljefors, T.; Krosgaard-Larsen, P. Neuronal nicotinic acetylcholine receptors: structural revelations, target identifications, and therapeutic inspirations. *J. Med. Chem.* **2005**, *48*, 4705–4745.

(33) Navarro, H. A.; Xu, H.; Zhong, D.; Abraham, P.; Carroll, F. I. In vitro and in vivo characterization of [<sup>125</sup>I]iodomethyllycaconitine in the rat. *Synapse* **2002**, *44*, 117–123.

(34) D'Amour, F. E.; Smith, D. L. A method for determining loss of pain sensation. *J. Pharmacol. Exp. Ther.* **1941**, *72*, 74–79.